Journal of Medicinal Chemistry

Article

pubs.acs.org/jmc

Conformationally Defined Rexinoids and Their Efficacy in the Prevention of Mammary Cancers

Venkatram R. Atigadda,[†] Gang Xia,[†] Anil Deshpande,[†] Lizhi Wu,[‡] Natalia Kedishvili,[‡] Craig D. Smith,[§] Helen Krontiras,[∥] Kirby I. Bland,[∥] Clinton J. Grubbs,[∥] Wayne J. Brouillette,*[,†] and Donald D. Muccio*[,†]

Departments of [†]Chemistry, [‡]Biochemistry and Molecular Genetics, [§]Vision Sciences, and [∥]Surgery, University of Alabama at Birmingham, Birmingham, Alabama 35294, United States

Supporting Information

ABSTRACT: (2*E*,4*E*,6*Z*,8*Z*)-8-(3′,4′-Dihydro-1′(2*H*)-naphthalen-1′-ylidene)-3,7-dimethyl-2,3,6-octatrienoinic acid (UAB30) is currently undergoing clinical evaluation as a novel cancer prevention agent. In efforts to develop even more highly potent rexinoids that prevent breast cancer without toxicity, we further explore here the structure−activity relationship of two separate classes of rexinoids. UAB30 belongs to the class II rexinoids and possesses a 9*Z*-tetraenoic acid chain bonded to a tetralone ring, whereas the class I rexinoids contain the same 9*Z*-tetraenoic acid chain bonded to a disubstituted cyclohexenyl ring. Among the 12 class I and class II rexinoids evaluated, the class I rexinoid **11** is most effective in preventing breast cancers in an in vivo rat model alone or in combination with tamoxifen. Rexinoid **11** also reduces the size of established tumors and exhibits a therapeutic effect. However, **11** induces hypertriglyceridemia at its effective dose. On the other hand rexinoid **10** does not increase triglyceride levels while being effective in the in vivo chemoprevention assay. X-ray studies of four rexinoids bound to the ligand binding domain of the retinoid X receptor reveal key structural aspects that enhance potency as well as those that enhance the synthesis of lipids.

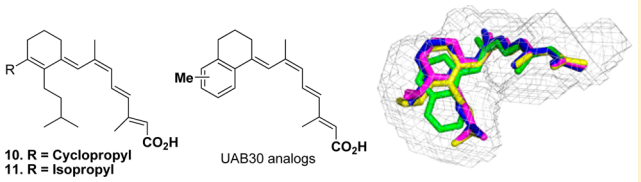

1. INTRODUCTION

Rexinoid agonists target exclusively the retinoid X receptors (RXRs) over agonists for the retinoic acid receptors (RARs). Bexarotene (Targretin) is the only clinically used rexinoid approved by the FDA (Figure 1). UAB30 is a rexinoid that is derived from the structure of 9-*cis*-retinoic acid, except it contains a tetralone ring connected to a 9*Z*-tetraenoic acid side chain. Recently the X-ray structures of each of these rexinoids were determined bound to the ligand binding domain of the human retinoid X receptor (hRXRα-LBD). Each rexinoid adopts an L-shaped conformation, which is characteristic of the way rexinoid agonists or the pan-agonist 9-*cis*-retinoic acid binds to the receptor.[1,2] The binding of the rexinoid agonists cause similar, but not identical, conformational and dynamical changes to the ligand binding domain enabling the recruitment of an amphipathic coactivator peptide containing the LLxxLL motif. Each rexinoid reduces proliferation and enhances apoptosis in mammary tumors and efficiently prevents mammary cancers in rodent models.[3−5] Hyperlipidemia is the dose-limiting toxicity of bexarotene in humans.[6,7] Genomic, proteomic, and metabolomics studies establish that oral dosing of bexarotene induces triglyceride synthesis in rat livers by hyperstimulating transcription of genes under the control of the RXR:LXR heterodimer, but oral dosing of UAB30 does not.[8,9]

To improve upon the potency of UAB30, a series of UAB30 homologues were generated with a single methyl group added to the carbon positions of the tetralone ring.[10,11] The monomethyl substituted UAB30 homologues **1**−**5** are more potent than UAB30, likely because of the increased lipophilic interactions between the ligands and the hydrophobic residues that line the ligand binding pocket of hRXRα-LBD. Oral dosing of two methyl homologues of UAB30, **1** and **4**, substantially increases the synthesis of triglycerides in the liver and accumulation in serum when orally administered to rodents. The enhanced levels of triglycerides observed in the serum after oral administration of **1** or **4** are similar to those found when bexarotene is administered. In contrast to these methyl homologues, the methyl substitution of UAB30 at other positions of the tetralone produces rexinoids **2**, **3**, and **5** that are more potent agonists than UAB30 without stimulating accumulation of triglycerides in the serum.[11] The X-ray crystallography structure of **1** or **4** bound to the hRXRα-LBD revealed that the methyl groups on the tetralone ring interacts strongly with helix 7 residues, Phe346 and Val349; whereas the methyl groups of the tetralone rings of **2**, **3**, and **5** did not interact with these residues. Furthermore, two methyl groups of the bexarotene tetrahydronaphthalene occupy the same space in the binding pocket as the methyl groups of **1** and **4**. Prior studies suggest that RXR potency can be separated from lipogenic toxicity by avoiding these interactions.[9,11] In this study we prepare each monomethyl homologue of UAB30 in multigram levels and evaluate them for their capability to prevent mammary cancers in rats initiated by the potent carcinogen, 1-methyl-1-nitrosourea (MNU). This study also explores the ring-expanded homologue of UAB30, **6**, which contains a benzosuberone ring bonded to a 9*Z*-tetraenoic acid side chain.

Received: May 29, 2015

DOI: 10.1021/acs.jmedchem.5b00829
J. Med. Chem. XXXX, XXX, XXX−XXX

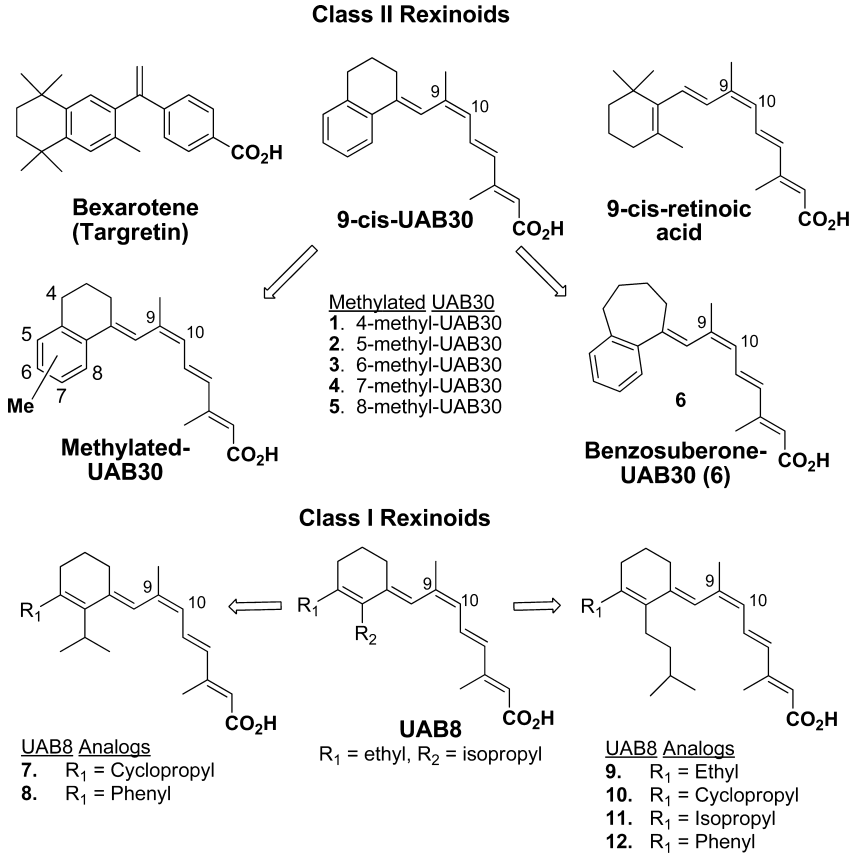

Figure 1. (Top) Structures of bexarotene and 9-*cis*-retinoic acid. Structures of class II rexinoids: UAB30, five methyl homologues of UAB30 **1**–**5**, and a benzosuberone homologue of UAB30, **6**. (Bottom) Structure of class I rexinoid: UAB8 and six more highly substituted analogs of UAB8 (**7**–**12**).

Scheme 1. Synthesis of New Class I UAB Rexinoids (9–12) with Different Substituents at R_1

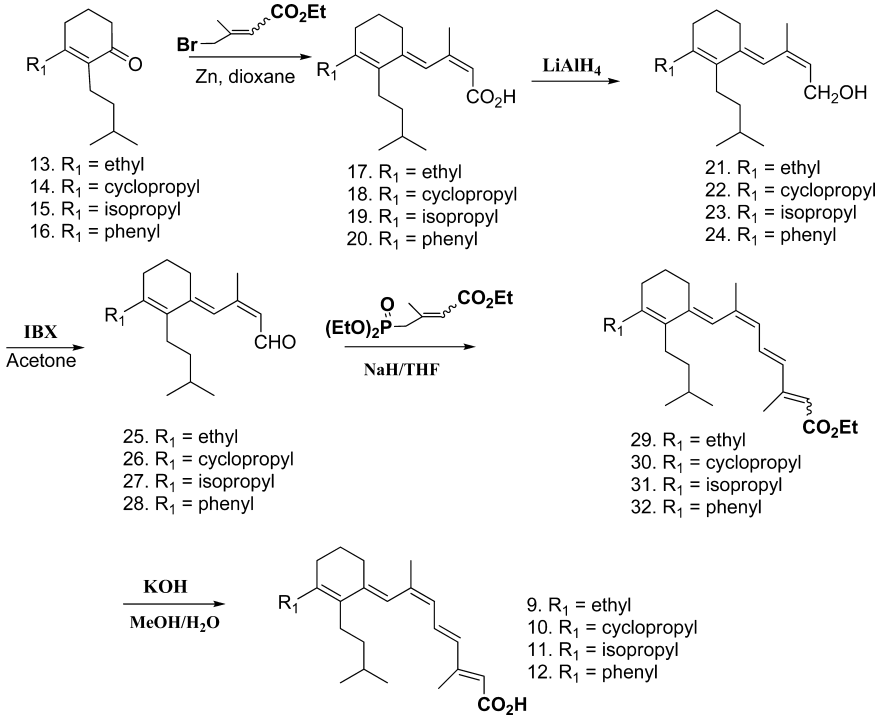

The larger ring of **6** is expected to interact better with the ligand binding pocket residues (particularly helix 11 residues) while providing minimal interaction to the helix 7 residues that are thought to induce triglyceride biosynthesis.

DOI: 10.1021/acs.jmedchem.5b00829
J. Med. Chem. XXXX, XXX, XXX−XXX

Table 1. Summary of Biological Data for UAB Rexinoids, Bexarotene, and 9-*cis*-Retinoic Acid

rexinoid or pan-agonist	RXRα binding, K_d (nM)	RXRα activation, EC_{50} (nM)	increase in serum triglyceride, 200 mg/kg diet (%)	reduction in cancer,[c,d] 200 mg/kg diet (unless otherwise noted) number (%)	weight (%)
9-*cis*-RA	14 ± 3[b]	120 ± 30[b]	326[a]	65[a]	90
bexarotene	26 ± 3[b]	40 ± 3[b]	456[b]	70[b]	76
UAB30	33 ± 5[b]	820 ± 70[b]	63[a]	63[a]	76[a]
1	25 ± 5[b]	120 ± 5[b]	560[b]	78	72
2	18 ± 3[b]	720 ± 20[b]	31[b]	0	0
3	15 ± 2[b]	100 ± 30[b]	51[b]	10	>10
4	8 ± 2[b]	160 ± 10[b]	642[b]	61, 100 mg	51
5	10 ± 1[b]	620 ± 50[b]	59[b]	0	0
6	9 ± 3	30 ± 5	175	30	33
7	34 ± 10	50 ± 5	289	43	32
8	125 ± 25	215 ± 30	6[b]	15[b]	21
9	14 ± 3	23 ± 5	341	69	86
10	35 ± 4	19 ± 5	71	62	64
11	9 ± 3	22 ± 5	430	99	96
12	150 ± 10	80 ± 15	76[b]	1[b]	27↑

[a]Data reported by Grubbs et al.[3,11] using 150 mg/kg diet of bexarotene, 60 mg/kg diet of 9cRA, and 200 mg/kg diet for 9cUAB30. [b]Data reported in Atigadda et al. and Deshpande et al.[10,11] for 150 mg/kg diet for Targretin and 200 mg/kg diet for (*R*)-4-Me-UAB30. [c]The percent reduction is cancer is determined as [(number of cancers in rats fed control diet − number of cancers in rats fed control diet plus test rexinoid)/(number cancers in rats fed control diet)] × 100. [d]Methods are described refs 5 and 8.

To continue to explore the relationship between potency and lipid toxicity, class I UAB rexinoids are revisited. Class I rexinoids contain a disubstituted cyclohexenyl ring bonded to the 9*Z*-tetraenoic acid side chain rather than the substituted tetralone ring (Figure 1). Previously, we produced UAB8, which contains an ethyl group at R_1 and isopropyl group at R_2 of the cyclohexenyl ring.[12,13] The 9-*cis*-isomer of UAB8 displayed RXR-selectivity with potency that approaches that of the pan-agonist 9-*cis*-retinoic acid.[12,13] Using structural information on the ligand binding pocket of RXR containing UAB30, methyl homologues of UAB30, bexarotene, and 9-*cis*-retinoic acid, we predicted that analogs of UAB8 containing larger alkyl groups at R_1 and R_2 can be introduced into the generic structure of class I rexinoids (Figure 1).

In the second part of this study, we prepare a series of class I rexinoids **7**−**12** to understand how steric bulk at the cyclohexenyl ring affects agonist potency and activity as a preventive agent. We identify the class I rexinoid **11** (R_1 = isopropyl group; R_2 = isopentyl group) which is substantially more potent than 9-*cis*-retinoic acid and even exceeds the potency of bexarotene. We determine X-ray crystal structures of hRXRα-LBD bound to **9**, **10**, or **11** to provide information on the key interactions in the ligand binding pocket that controls potency. As with class II rexinoids, the newly designed class I rexinoids, **7**−**12**, are synthesized at multigram levels for evaluation in 90-day chemoprevention assays for mammary cancer prevention. This affords us a comparison of the efficacies of each class of rexinoids as potential drugs to prevent mammary cancer.

2. RESULTS AND DISCUSSION

2.1. Chemistry. Rexinoids **1**−**5** were synthesized at the 30 g levels using the previously reported methods to generate smaller quantities.[10,11] Rexinoid **1** was synthesized using commercially available racemic 4-methyltetralone. Rexinoid **6** was synthesized utilizing the same methodology starting from benzosuberone rather than tetralones. The detailed experimental procedure is provided in the Supporting Information. Rexinoids **7** and **8** were synthesized using methods that were described previously for UAB8; the detailed experimental procedures are also provided in the Supporting Information. Scheme 1 summarizes the syntheses of the retinoids **9**−**12**. The starting ketones (**13**−**16**) with the appropriate substituents at R_1 and R_2 were synthesized using previously reported methods, and the detailed experimental procedures for these precursors are provided in the Supporting Information.[12,13] The synthesis of retinoids **9**−**12** began with a Reformatsky reaction between the ketones **13**−**16** and ethyl 4-bromo-3-methyl-2-butenoate (1:1 mixture of isomers) in 1,4-dioxane to provide the 9*Z*-acids **17**−**20** in 70−85% yield. The carboxyl groups in compounds **17**−**20** were then reduced in the presence of $LiAlH_4$ to produce the desired 9*Z*-alcohols **21**−**24** in quantitative yield. The alcohol functional groups in compounds **21**−**24** were next oxidized using IBX[14] (rather than MnO_2) to provide the desired 9*Z*-aldehydes **25**−**28** containing minor amounts of all *E*-aldehyde (5−7%). Pure 9*Z*-isomers (**25**−**28**) were isolated in 65−80% yields following column chromatography. Olefination of aldehydes **25**−**28** in the presence of triethyl phosphonosenecioate (1:1 mixture of isomers) under Horner−Emmons conditions provided the esters **29**−**32** as an 85:15 mixture of the 9*Z*-isomer to the 9*Z*,13*Z*-isomer. Since the two isomers were not separable by column chromatography, hydrolysis of the esters in compounds **29**−**32** was performed on the mixture of 9*Z* and 9*Z*,13*Z*-isomers under basic conditions to provide the acids **9**−**12**. The desired pure 9*Z*-isomers **9**−**12** were obtained after recrystallization in 60−65% yields.

2.2. Binding and Transactivation of Rexinoids to RXR. In our previous publications we determined the dissociation constants (K_d) for retinoid-receptor complexes by using a fluorescence quenching method.[1,10,11] By use of this method, the K_d values for the dissociation of either 9-*cis*-retinoic acid or UAB30 from its complex with the hRXRα-LBD homodimer were determined to be 14 and 33 nM, respectively (Table 1).[1] Fluorescence titrations of rexinoids **1**−**5** demonstrated each methyl homologue was a better binder to hRXRα-LBD than UAB30 (Table 1). By use of the same method, **6**−**12** were evaluated for binding to hRXRα-LBD. Rexinoids **6**, **7**, and **9**−**11**

DOI: 10.1021/acs.jmedchem.5b00829
J. Med. Chem. XXXX, XXX, XXX−XXX

Table 2. Summary of ITC Measurements of GRIP-1 Binding to hRXRα-LBD:Rexinoid Complexes at 25 °C

rexinoid (25 °C)	K_d (μM)	ΔH (kcal/mol)	$-T\Delta S$ (kcal/mol)	ΔG (kcal/mol)	n
9-*cis*-retinoic acid	1.81 ± 0.06	−9.2 ± 0.03	0.61 ± 0.06	−8.5 ± 0.03	0.92
UAB30	1.33 ± 0.12	−8.9 ± 0.03	0.52 ± 0.12	−8.4 ± 0.03	1.05
bexarotene	1.59 ± 0.04	−9.5 ± 0.02	0.84 ± 0.04	−8.6 ± 0.12	0.96
11	1.21 ± 0.03	−9.4 ± 0.04	0.36 ± 0.03	−8.5 ± 0.06	0.93
12	0.47 ± 0.02	−7.6 ± 0.05	0.92 ± 0.05	−7.2 ± 0.05	0.96

quenched more than 90% of the protein fluorescence signal at 337 nm when the ratio of the protein to the rexinoids reached 1:1. Each of these rexinoids was a better binder to hRXRα-LBD than UAB30. Rexinoids **8** or **12** were the exception; they were 5-fold weaker binders than UAB30 to hRXRα-LBD.

Binding affinity to hRXRα-LBD is the simplest evaluation of the potential potency of the rexinoid. To evaluate the efficacy of rexinoids as agonists, the HEK293 cell line was transiently transfected with a Gal4 reporter construct containing the hRXRα-LBD. The enhancement of gene transcription mediated by agonist was measured using a luciferase reporter system. This cell line and reporter were recently used to compare the activities of UAB30, 9-*cis*-retinoic acid and bexarotene as well as comparing the agonist activities of different methyl homologues of UAB30.[10,11] Selective data from the previous studies are included in Table 1 so that the potencies of class II rexinoids can be compared to class I rexinoids and bexarotene. In this cell line bexarotene is 3-fold more potent as a RXR agonist ($EC_{50} \approx 40$ nM) than 9-*cis*-retinoic acid ($EC_{50} \approx 120$ nM). UAB30 is a 20-fold weaker agonist in this cell line than bexarotene, even though it was a potent agonist ($EC_{50} = 118$ nM) in the CV-1 cell line used previously.[4] Apparently, UAB30 does not recruit endogenous coactivator proteins in the HEK293 cell line as well as those found in CV-1 cells (coactivator types and abundance vary according to cell type). Given the demonstrated tissue-selective effects of this rexinoid, it is not suprising to find its potency changing with different in vitro evaluation conditions. Relative to these data, **6** was evaluated next. Rexinoid **6** is a closely related homologue of UAB30 containing an extra methylene group in the benzosuberone ring relative to the tetralone ring. Consistent with its potent binding to hRXRα-LBD, **6** was also a potent activator of RXR-mediated transcription, similar to that of bexarotene (Table 1). Rexinoid **7** is built on the cyclohexenyl ring scaffold (Figure 1). The EC_{50} value of **7** was similar to that of bexarotene. When the steric size of the R_1 substituent was increased to a phenyl group, the potency of **8** was substantially lost relative to **7**. The R_2 substituent of class I rexinoids was increased to an isopentyl group to give **9**. The potency of **9** was 2-fold better than that of **7**. The potencies of rexinoids **10** (R_1 = cyclopropyl) and **11** (R_1 = isopropyl) were similar to the potency of **9** (R_1 = ethyl). When the size of the R_1 was increased to a phenyl group, the potency of **12** was much poorer ($EC_{50} \approx 80$ nM) than those of **9**−**11**. Furthermore, the response at the 1000 nM dose was only 30% of that of **12**, suggesting that **12** is a partial agonist. This loss of agonist properties for **12** (R_1 = phenyl; R_2 = isopentyl) relative to **11** (R_1 = isopropyl; R_2 = isopentyl) was similar to the loss of activity of **8** relative to **7**. The EC_{50} value of **12** was 10-fold less than those of **9**−**11**. Rexinoid **12** was a partial agonist in this cell line inducing only 20% of the signal of 9-*cis*-retinoic acid at 1000 nM. When RARα activation was examined, rexinoids **1**−**6** and **12** did not activate transcription relative to controls (less than 5%) at 10^{-6} M; rexinoids **5**, **9**−**11** induced 20% activation of RARα-mediated transcription at 10^{-6} M.

For the RXR full agonists 9-*cis*-retinoic acid, UAB30, several methyl analogs of UAB30 or bexarotene, the thermodynamic parameters determined from ITC titration of the coactivator peptide GRIP-1 into hRXRα-LBD homodimers saturated with agonist were similar regardless of structure of the rexinoid agonist in the ligand binding pocket.[4,5,7] In this study, we compared the thermodynamics of GRIP-1 binding to hRXRα-LBD homodimers containing the full and potent agonist, **11**, to that of the partial agonist, **12**. This comparison was undertaken to decide if the partial agonist, **12**, was capable of recruiting coactivator peptide to the surface of the RXR receptor like other structurally different full agonists. Isothermal titration calorimetry (ITC) measurements were performed at 25 °C (Table 2). When 9-*cis*-retinoic acid, UAB30, or bexarotene was bound to hRXRα-LBD homodimers, GRIP-1 bound well to each coactivator binding site on the monomers (stoichiometry of nearly 1 for GRIP-1:hRXRα-LBD monomer subunit). For **11**, the stoichiometry for GRIP-1 binding was also 1. The binding affinities, binding enthalpies, entropies, or free energies of GRIP-1 to the full agonist bound complexes were nearly identical to each other (Table 2). This indicates that hRXRα-LBD homodimers containing **11** adopt a similar surface on the LBD to recruit coactivators as found in RXR homodimers containing other potent agonists. The thermodynamic signature of coactivator binding is a necessary but not sufficient property of a potent agonist. The binding of GRIP-1 to hRXRα-LBD homodimers containing **12** was different from those found from all other ITC studies. The binding affinity of GRIP was 3-fold less as was reflected in the 1 kcal/mol lower free energy of binding (−7.2 kcal/mol). The negative free energy change for GRIP-1 binding to the receptor complex bound with **12** was still present, but the enthalpy change was substantially smaller in magnitude than observed for the full agonists studied (−7.6 kcal/mol versus −9.4 kcal/mol). The change in enthalpy may be a thermodynamic signature for GRIP-1 binding to homodimers containing full agonists versus partial agonists, and it may be used as a rapid screen for partial agonists of the RXR receptor.

2.3. Crystal Structures of hRXRα-LBD Homodimers Bound with Rexinoids 6, 9, 10, or 11. The X-ray crystal structures of hRXRα-LBD homodimers bound to the pan-agonist 9-*cis*-retinoic acid or RXR-selective agonists, bexarotene, UAB30, and its methyl analogs with coactivator peptide GRIP-1 (^{686}KHKILHRLLQDSS^{698}) were valuable to understanding structural factors that influenced biological activity and toxicity.[1,2,10] Here crystal strutures of hRXRα-LBD homodimers containing the coactivator peptide GRIP-1 with one of four potent agonists (**6**, **9**, **10**, and **11**) were obtained and compared. Crystals of the homodimer containing the partial agonist **8** or **12** were not successfully obtained after repeated tries using similar conditions of crystallization to those of full agonists. In our laboratory, 13 crystals of hRXRα-LBD homodimers each containing a potent rexinoid agonist and GRIP-1 were generated using similar crystallization conditions, suggesting that these conditions are suited to generate crystals of homodimers bound

DOI: 10.1021/acs.jmedchem.5b00829
J. Med. Chem. XXXX, XXX, XXX−XXX

to full RXR agonists but not for the crystallization of homodimers bound to partial agonists. Each crystal structure of hRXRα-LBD homodimers containing GRIP-1 and either agonist **6** or **9**–**11** belonged to the $P4_{(3)}2_{(1)}2$ space group. The unit cell contained two monomers of LBD with GRIP-1 bound to each monomer. The summary of the X-ray crystallography and refinement statistics for the structures is listed in a table provided in the Supporting Information.

The 3D fold of the hRXRα-LBD homodimer was nearly identical to previously reported structures.[2] The backbone atoms of each structure were overlaid with the structure of hRXRα-LBD bound to UAB30 and GRIP-1 complex (4K4J). The rmsd values for this overlay of 229 backbone residues were 0.177, 0.211, 0.161, and 0.166 Å for homodimers bound to **6**, **9**, **10**, and **11**, respectively (Figure 2). Four conformational changes occurred

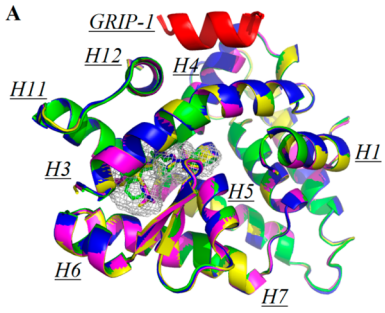

Figure 2. Overlay of X-ray crystal structures of hRXRα-LBD bound to UAB30 (PDB code 4K4J), **6** (PDB code 4RFW), **9** (PDB code 4RMC), **10** (PDB code 4RMD), **11** (PDB code 4RME). The coactivator peptide GRIP-1 is displayed in red, and the ligand binding pocket of hRXRα-LBD is highlighted in gray mesh.

in the layer between the rexinoid binding site and the coactivator binding site when GRIP-1 binds to holo-protein complex.[1,2,11] These conformational changes allow helix 12 of the hRXRα-LBD to form and stabilize the coactivator binding site. Each of these conformational changes were observed in the structures of hRXRα-LBD containing **6**, **9**, **10**, or **11**. Together with helices 3 and 4 residues, the ILxxLL motif of GRIP-1 bound to the hydrophobic pocket on the surface of the receptor and GRIP-1 was held by two charge clamps involving Glu453 of helix 12 and Lys284 of helix 3. The ITC study of the GRIP-1 binding to hRXRα-LBD with **11** is consistent with the structural data presented here. GRIP-1 binding to hRXRα-LBD containing the partial agonist **12** produced a different thermodynamic signature (weaker binding affinity and smaller negative enthalpy change) than observed when a full agonist, **11**, is bound. The change in thermodynamics of GRIP-1 binding to LBD complexes with **11** versus **12** supports the notion that the surface of the LBD complex when partial agonist **12** is bound is different from the surface when the full agonist **11** is bound.

2.4. Ligand Binding Pocket of hRXRα-LBD Containing Rexinoid 6, 9, 10, or 11. Rexinoids **6**, **9**, **10**, and **11** were well-defined by their electron density maps in the LBP of hRXRα-LBD. Each rexinoid adopted a nonplanar L-shape conformation that filled the ligand binding pocket of the LBD (Figure 3). The dihedral angles of C7–C8–C9–C10 of **6**, **9**, **10**, and **11** were 106.0°, 111.5°, 120.1°, and 100.9°, respectively. The dihedral angle of C7–C8–C9–C10 of **6** was twisted less than that of UAB30 (121.4°). Even with this change, the structures of **6** and UAB30 overlaid well (Figure 3A). The benzosuberone ring of **6** occupied the same space as the tetralone ring of UAB30, except it

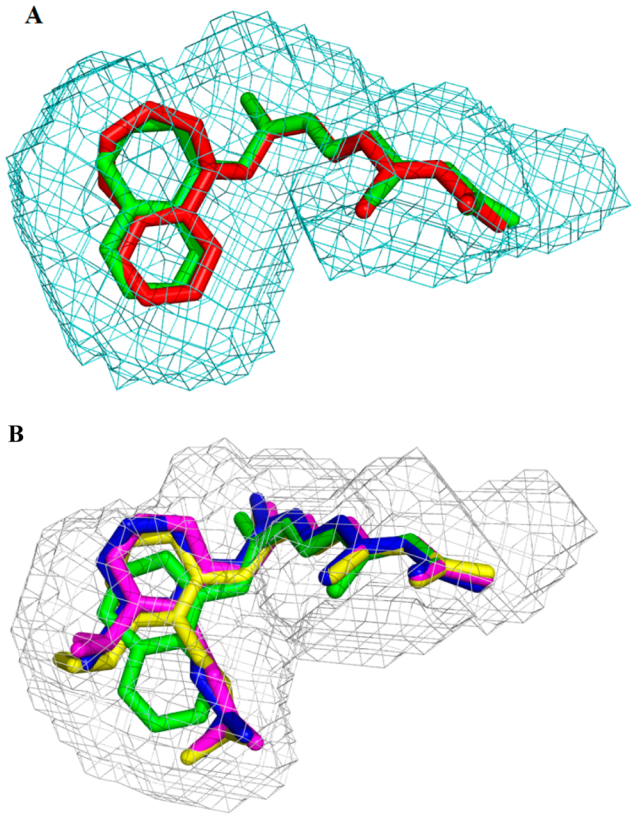

Figure 3. (A) Overlay of UAB30 (green, PDB code 4K4J) and class II UAB rexinoid, **6** (red, PDB code 4RFW) in the ligand binding pocket (gray). (B) Overlay of UAB30 (green, PDB code 4K4J) and class I UAB rexinoids, **9** (blue, PDB code 4RMC), **10** (yellow, PDB code 4RMD), and **11** (purple, PDB code 4RME) in the ligand binding pocket (gray).

was slightly less planar as expected for the seven-membered ring of the benzosuberone relative to the six-membered ring of the tetralone. The structures of **9**, **10**, and **11** occupied the ligand binding pocket in a very similar manner to each other, and these structures overlaid well with that of UAB30 (Figure 3B). The polyene chains of these rexinoids were nearly identical, and the substituted cyclohexenyl rings of each rexinoid were oriented in the same space as the tetralone ring of UAB30. The cyclohexenyl ring of **11** is tilted toward helix 11 residues more than rings of **9** and **10**. The cyclohexenyl rings of **9** and **10** were in an envelope conformation in which the C1′ and C2′ atoms are all on the opposite side of C19. The cyclohexenyl ring of **11** adopted a half-chair conformation with C1′ on the same side as C19 and with C2′ on the opposite side of C19. The extra space in the electron density map of the rexinoids at R_1 was limited. The phenyl group at R_1 of **12** could not occupy this space without disrupting the 3D fold of the protein, which provides a structural explanation for its partial agonist properties.

For structures studied in our laboratory, the ligand binding pocket is small when UAB30 is bound to hRXRα-LBD (442 Å^3). The ligand binding pocket of the RXR domain containing **6** was slightly larger (464 Å^3) than found for UAB30. The size of this pocket increased to 545 Å^3 to accommodate **9**, **10**, and **11**. Even though the size of the ligand binding pocket changed, the rexinoids each occupied 75% of available space. To examine changes in the geometry of the protein residues that surrounded the ligand, we provide electron density maps of each rexinoid focusing on the ring region of the ligand binding pocket (Figure 4A). Even though **6**, **9**, **10**, and **11** made more contacts with the

DOI: 10.1021/acs.jmedchem.5b00829
J. Med. Chem. XXXX, XXX, XXX–XXX

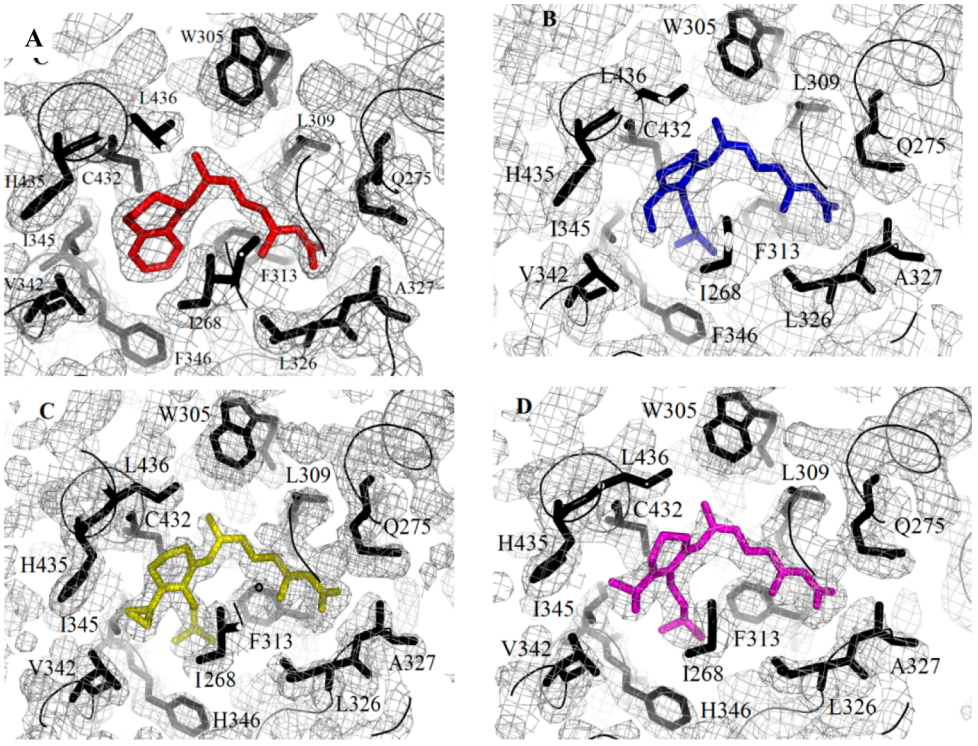

Figure 4. (A) Electron density maps ($2F_o - F_c$) for the ligand binding pocket containing **6** (PDB code 4RFW). (B) Electron density maps ($2F_o - F_c$) for the ligand binding pocket containing **9** (PDB code 4RMC). (C) Electron density maps ($2F_o - F_c$) for the ligand binding pocket containing **10** (PDB code 4RMD). (D) Electron density maps ($2F_o - F_c$) for the ligand binding pocket containing **11** (PDB code 4RME).

protein residues surrounding them in the ligand binding pockets of their complexes with hRXRα-LBD than found for the smaller UAB30, the protein residues that interact with these rexinoids were nearly identical to each other and to UAB30 (Figure 4A). For **6** relative to UAB30, the change in total contact surface area was only 25 Å^2. The polyene chain of **6** increased its contact to residues on helices 3 and 5 slightly more than found for UAB30. For **9**, **10**, and **11**, the total contact surface areas of the rexinoid to hRXRα-LBD were each about 100 Å^2 larger than those observed for 9cUAB30. In particular **9**, **10**, and **11** made more contacts with the protein residues of helices 3, 5, and 7 and the β sheet than either 9-*cis*-retinoic acid or UAB30 did. When helix 11 residues were examined, **9** and **10** made fewer contacts with these residues than either 9-*cis*-retinoic acid or UAB30, while the total contact surface area of **11** with helix 11 residues was similar to those found in UAB30. The ethyl, cyclopropyl, and isopropyl groups at R_1 of **9**, **10**, and **11** interacted with residues on helix 7. The isopropyl group of **11** had one methyl group pointed to Val342 of helix 7 and the other methyl group pointed to Phe439 and His436 of helix 11. The cyclopropyl group of **10** exhibited similar interactions with helix 7 and helix 11 residues, but the methylene groups of the cyclopropyl group provided less surface area for interaction than the methyl groups of the isopropyl group. The ethyl group of **9** pointed toward Val342 of helix 7.

In our prior publication we demonstrated how a single methyl substitution at carbon 7 of the tetralone ring of UAB30 (rexinoid **4**) substantially enhanced the agonist potency of this methyl derivative over its parent compound, but this enhanced potency was at the expense of substantially enhancing lipid biosynthesis.[11] For class II rexinoid **4**, the methyl group at carbon 7 interacted strongly with Phe346 and Val349 of helix 7. The methyl groups on the reduced naphthalene ring of bexarotene interacted with same residues on helix 7. The class II rexinoid **6** is situated in the ligand binding pocket in a nearly identical manner to UAB30 (Figure 3A contains an overlay of the two rexinoids). The benzosuberone of **6** did not make van der Vaals contacts with Phe346 and Val349 of helix 7 (Figure 4A). The ring of **6** was only slightly larger than the ring of UAB30 and did not contain methyl groups that protrude toward the helix 7 residues. In contrast to **6**, rexinoids **9**, **10**, and **11** contained an isopentyl group at R_2 of the cyclohexenyl ring. When these structures were overlaid with those of UAB30, the isopentyl group extended well beyond the space occupied by the tetralone ring of UAB30 (Figure 3B) and pointed toward helix 7 (Figure 4B–D). As shown in the $2F_o - F_c$ plots, the methyl groups in isopentyl substituent of **9**, **10**, and **11** made substantial van der Waals contact with both Phe346 and Val349 of helix 7 (Figure 4B–D). Additionally an isopentyl methyl group interacted well with Phe313 of helix 5. This interaction was not present in **6** or UAB30; in these structures the methine at carbon-8 of the tetralone ring of UAB30 was just outside of van der Waals contact to Phe313. In the published structure of bexarotene, the methyl groups of the tetrahydronaphthalene ring interacted strongly with Phe313.[2] Rexinoids **9**, **10**, and **11** are as potent as or more potent than bexarotene as a RXR agonist in the in vitro transient transfection assays, which is consistent with the enhanced contacts between its ring R-groups and helix 7 (Table 1).

2.5. In Vivo Triglyceride Levels and Effectiveness for the Prevention of MNU-Initiated Mammary Cancer. Elevated serum triglyceride levels were observed in humans orally administered bexarotene or 9-*cis*-retinoic acid. The triglyceride levels measured in humans were similar to those found in rats given these drugs.[7] A 7-day in vivo screen was used to evaluate if oral dosing of other rexinoids (**6**–**12**) increases serum triglyceride levels. Serum triglycerides were measured in rats fed each rexinoid at a dose of 200 mg rexinoid/kg diet for 7

DOI: 10.1021/acs.jmedchem.5b00829
J. Med. Chem. XXXX, XXX, XXX−XXX

days. As displayed in Table 1, class I rexinoids **8**, **10**, and **12** did not significantly increase triglycerides over control rodents. The modest increase in serum triglyceride levels measured for either **8** or **12** is consistent with their status as a partial RXR agonists. However, rexinoid **10** is a potent full agonist, yet triglyceride levels were low. Three class II rexinoids (**2**, **3**, and **5**) are other examples of potent agonists that did not increase serum triglycerides significantly above normal. Rexinoid **6** is a full agonist with similar potency to **10**; it elevated serum TG levels to 175% which is higher than those of UAB30, **2**, **3**, **5**, or **10** but well below levels of bexarotene, 9-*cis*-retinoic acid, **1**, and **4**. Rexinoids **7**, **9**, and **11** are even more potent agonists than the class II rexinoids, and their administration raised triglycerides levels by 280−640% over controls, which are serum levels achieved when 9-*cis*-retinoic acid, bexarotene, **1**, or **3** is administered. Compared to the large increase seen with the 200 mg/kg dosing, a 100 mg/kg diet dose of **9** or **11** resulted in a smaller increase in serum triglyceride levels (about 1/2 the value observed for 200 mg/kg diet dosing). The structures of **9** and **11** contained methyl groups that interact strongly with helix 7 residues. These interactions were similar to those observed for **1**, **4**, or bexarotene.[10,11] Thus, each rexinoid that contained these structural features increased lipid biosynthesis and accumulation in serum. Unexpectedly, **10** with an isopentyl group at R_2, which interacted with helix 7 residues, did not substantially raise serum TG levels. As discussed previously, there were subtle differences in structure of **10** versus **11** in the ligand binding pocket. The cyclopropyl group at R_1 of **10** apparently influenced agonist activity as well as mitigated lipid biosynthesis.

The NCI Division of Cancer Prevention uses the MNU-initiated mammary model to evaluate the potential of new compounds for the prevention of ER-positive breast cancers in humans. Recent gene array studies revealed that aromatase inhibitors modulated gene products in the MNU-chemically initiated model for mammary cancer in rats that were remarkably similar to how these drugs modulated gene products in humans with ER-positive breast cancers.[15] Like aromatase inhibitors, rexinoid agonists prevented chemically initiated mammary cancers in this rat model. We demonstrated that UAB30 or racemic **1** was as effective as 9-*cis*-retinoic and bexarotene in preventing cancers in the MNU model (Table 1).[1,2,10] In this study, we evaluated the efficacy of both class I and class II rexinoids in the same 3-month model that informs on the preventive effects of new drugs in humans. The effectiveness of class I and class II rexinoids reported in Table 1 are reported at a single dose of 200 mg/kg diet, which was used for the evaluation of UAB30 (except for **4** as discussed later). After 3 months of treatment at 200 mg/kg diet after carcinogen administration, **11** was clearly the most effective rexinoid; it was even more effective than bexarotene. Rexinoid **11** prevented essentially all mammary cancers at this dose without overt toxicity (except elevated lipids). Rexinoids **9** and **10** were also effective in preventing 60−70% of mammary cancers. Rexinoid **7** had intermediate effectiveness and reduced only 43% of cancers, which is less than the more potent class I rexinoids, **9**, **10**, or **11**. Rexinoids **8** and **12**, two partial agonists, exhibited no effectiveness in the prevention of mammary cancers. The effectiveness of cancer prevention clearly correlated with agonist potency for class I rexinoids.

Among class II rexinoids, only two methyl homologues of UAB30 were as effective or more effective than UAB30. Rexinoid **1** was slightly more effective than UAB30, consistent with its enhanced agonist potency. Rexinoid **4** was effective but particularly toxic to rats when evaluated in the MNU-initiated prevention model using a 200 mg/kg diet dose. After a month of chronic treatment at this dose, rats displayed clinical signs of hypervitaminosis A toxicity (e.g., reduction of body weight gain, skin reddening, and mucus membrane dryness). The dose was lowered to 100 mg/kg diet after toxicity was observed, and the study was continued to duration without further clinical observation of vitamin A toxicity. Essentially no tumors appeared at the termination of the study in the treated group. To further evaluate the effectiveness of this rexinoid, **4** was evaluated again in this prevention model using a 100 mg/kg diet dose for the entire 3 months of study. Rexinoid **4** was 61% effective at the lower dose (Table 1). Serum triglycerides were elevated by 350% in rat serum when fed the 100 mg/kg diet. The UAB30 methyl homologues **2**, **3**, and **5** and rexinoid **6** were not effective (or poorly effective) at the 200 mg/kg diet dose. The low effectiveness of **2**, **3**, **5**, or **6** as preventative agents was surprising. For class I rexinoids the effectiveness as an RXR agonist correlated well with its effectiveness in cancer prevention, but this correlation was not observed for **2**, **3**, **5**, or **6** (Table 1). To evaluate metabolism, the serum levels were measured after the study. The serum levels of **1**, **2**, **3**, **5**, and **6** were well below 1 μM, which were much lower than observed for UAB30 (2 μM). The serum levels of every class I rexinoids were 3 μM or greater (3−6 μM). The low serum levels of **2**, **3**, and **5** suggest that oxidative metabolism (e.g., benzylic oxidation of methyl groups) may play a role in the reduced potency of these rexinoids. Of those rexinoids examined in our laboratory, only the pan-agonist 9-*cis*-retinoic acid prevents mammary cancers in this rodent model when serum levels are low (<1 μM). Every other active rexinoid in this mammary model exhibited higher serum levels in excess of 1 μM.

The preventive effects of **11** encouraged us to continue its evaluation as a putative preventive agent for mammary cancer. We undertook a study using lower doses alone and in combination with the selective estrogen receptor modulator (SERM) tamoxifen. When **11** was administered at 50 mg/kg diet, cancer incidence was 26% alone (decrease in tumor size was 37%). With a 0.4 mg/dg diet dose of tamoxifen, the cancer incidence in this group of rats was 10% (decrease in tumor size was 3%). When rats were fed the low-dose **11** and tamoxifen together, the cancer incidence was 53% after 120 days (decrease in tumor size was 68%), which suggested an additive or synergic effect of preventive actions of the SERM and rexinoid. As importantly, the lower dose of **11** only increased serum TG by about 65% (substantially lower than a 200 kg/diet dose). The lower dose is more viable for use as a potential preventive agent in the clinic, since lipid toxicity would be less of a problem for long-term administration. These studies were similar to those published for 9-*cis*-retinoic acid, UAB30, or bexarotene using a lower dose.[3,8]

2.6. Inhibition of Growth of MNU-Initiated Mammary Tumors. SERMs are administered to humans with ER-positive mammary cancers in an adjuvant or neoadjuvant setting in the clinic. Since rexinoids reduce proliferation in existing MNU-initiated mammary cancers, we next investigated if rexinoid treatment would slow the growth of existing mammary tumors. To investigate the effectiveness of rexinoids for therapy of ER-positive mammary cancers, rats (N = 9) with small MNU-initiated tumors of about 200 mm^2 were treated with 200 mg/kg diet of UAB30 or with **11**. The size of mammary tumors in control animals rapidly grew. The rate of tumor growth was different for each animal, which is consistent with chemically

DOI: 10.1021/acs.jmedchem.5b00829
J. Med. Chem. XXXX, XXX, XXX−XXX

induced tumors containing different genomic instabilities. To account for slightly different sizes of tumors at day 0, the data were normalized to the size of the tumor at day 0 (just prior to rexinoid administration). The change in the size of a tumor with time is reported as a percent change relative to the size of the tumor at day 0. After 7 days of rexinoid treatment, the average tumor size of the untreated group nearly doubled. After 14 days, the tumors from control group rats were on average 4-fold larger (Figure 5). At this time point one rat was removed from the study

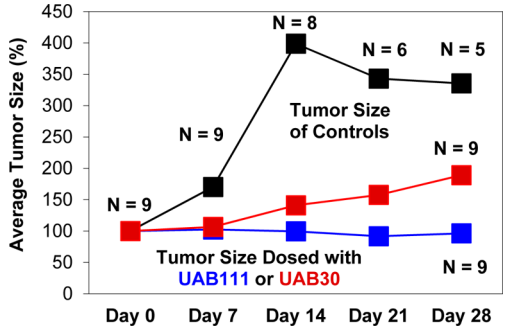

Figure 5. Treatment of small existing MNU-initiated rat mammary cancers with UAB30 (red) or class I rexinoid, **11** (blue), at 200 mg/kg diet versus controls (black). The size of the mammary cancers was normalized to 100% at day zero of treatment ($N = 9$). The change of the size of the cancer for controls or treated rats were measured once a week for 4 weeks and averaged at each time point. The average tumor size (y-axis) was determined by the ratio of the average size at the indicated day to the average size at day zero. Nine animals ($n = 9$) survived in each treated group, and five animals ($n = 5$) survived in the control group after 28 days.

to prevent death from a large necrotic tumor. At later time points, especially rapid tumor growth resulted in removal of three additional rats from the study in the control group to avoid death. The average size of the tumors was smaller at time points of 21 and 28 days because of the smaller average size of the remaining tumors in control rats (since these are chemically initiated spontaneous tumors with different genetic mutations, tumors grow at different rates). In contrast to tumors from rats fed only control diets, the average tumor size of rats fed **11** mainly decreased after 28 days of treatment (Figure 5). In one rat, the tumor completely disappeared at day 24; in four other animals the tumor size significantly decreased after 28 days of treatment with **11** (30−55% decrease in size). In only one treated rat, the tumor growth was similar to that in the control rats. These data demonstrate that treatment with **11** is capable of regressing tumor growth for many cancer genotypes. The preclinical studies suggest **11** could be used as an adjuvant or neoadjuvant agent of estrogen-positive tumors in addition to its use to prevent new cancers. A similar effect was observed for bexarotene treated MNU-mammary cancers.[8] UAB30 was also studied, since this is the most potent and least toxic rexinoid we have developed. The average size of tumors from rats treated with UAB30 increased slightly relative to day 0 (40% increase in the average size of tumors between day 0 and day 14), but tumors from control rats were 400% larger during the same time period (Figure 5).

3. CONCLUSIONS

The MNU-initiated mammary model is used currently by the NCI to identify new preventive breast cancer drugs. Recent studies demonstrate that the genomic changes observed in MNU-initiated mammary cancers from rats treated with aromatase inhibitors are similar to those observed in humans treated with the same class of drug.[15] Aromatase inhibitors block cell proliferation by downregulation of numerous genes (e.g., cyclins). Rexinoids (bexarotene or UAB30) display significant capability to prevent MNU-initiated mammary cancers; they significantly decrease cell proliferation in MNU-initiated cancers as well as increase apoptosis.[3,5,6,8] As reviewed by den Holannder et al.,[16] the RAR:RXR heterodimer is an important target of rexinoids. Retinoic acid, which is synthesized by oxidative metabolism of vitamin A, binds to RAR:RXR heterodimers, slows tumor cell proliferation, induces cell differentiation, and enhances apoptosis.[17] RXR agonists are known to enhance signaling of retinoic acid or other RAR agonists through the permissive RAR:RXR heterodimer. Bexarotene induces RXR and RAR expression in normal mammary epithelial cells and mammary cancers (T47D).[18] Bexarotene also stimulates the expression of insulin-like growth factor binding protein 6 and reduces cell proliferation and increases apoptosis.[18] Rexinoids have an added advantage of stimulating additional signaling pathways that control cell proliferation besides those pathways mediated by the RAR:RXR heterodimers. In vitro studies suggest rexinoids also enhance PPARγ:RXR signaling, which kill cancer cells. Studies by Bonofiglio et al. demonstrate profound effects of low doses of RXR and PPARγ agonists in inducing apoptosis in human breast cancer cells but not in normal breast epithelial cells.[19] This suggests that rexinoids may in fact be preventing mammary cancer by working with endogenous PPARγ agonists. Other recent work suggests PPARγ agonists and rexinoids work synergistically to block inflammatory signaling in cancer stem cells that surround and support growth of breast tumors.[20] Rexinoids (e.g., bexarotene) may also prevent mammary cancer development by suppressing the expression of COX-2 in normal and premalignant mammary epithelial cells.[21] We are still unsure if the profound effects that rexinoids have in the prevention of cancer are due to slowing growth and inducing cell death in microscopic disease (transformed tissue) or if these effects are due to preventing transformed epithelial cells from progressing from normal phenotypes to frank cancers. It is quite possible each rexinoid has different modes of action, even though they bind with high affinity to the same RXR receptor.

As the answer to this question emerges, we focus here on the clinical utility of a limited set of class I and II rexinoids. We search for a nontoxic rexinoid with clinical potential greater than that of UAB30, which is in clinical development for breast cancer prevention. Among class II rexinoids, we examined methyl homologues of UAB30, **1**−**5**, and a ring expanded rexinoid, **6**. Even though rexinoids **1**−**6** were substantially more potent than the parent RXRα agonist, UAB30, only two class II rexinoids, **1** and **4**, were more effective than UAB30, and each of these rexinoids produced substantial triglyceride accumulation in serum (a hallmark of lipid toxicity). Since cancer prevention in the high-risk population requires chronic dosing for extended periods (or even lifetimes), toxicity is a real concern in drug development. Among class II rexinoids, UAB30 is the clear compromise between reasonable effectiveness and low toxicity. We also examined rexinoids built from our original design of class I rexinoids. To date, UAB8 was the most potent homologue among this class reported.[12] Our recent structures of hRXRα-LBD containing bound class II rexinoids and bexarotene revealed that larger groups could be accommodated in the binding pocket of the LBD.[1,2,10,11] The most potent class I rexinoid contained an isopentyl group at R_2 and smaller alkyl groups (cyclopropyl or isopropyl) at R_1. Rexinoid **11** was substantially more potent than

DOI: 10.1021/acs.jmedchem.5b00829
J. Med. Chem. XXXX, XXX, XXX−XXX

bexarotene, and it exhibited an extremely high effectiveness to prevent mammary cancer. The structural studies revealed in this study demonstrated the isopentyl group at R_2 filled the ligand binding pocket optimally. Rexinoid **11** also demonstrated therapeutic potential at doses well below its cytotoxic effects. The increase in potency of **11** came at a cost. Rexinoid **11** exhibited enhanced triglyceride biosynthesis and accumulation in serum levels similar to bexarotene or 9-*cis*-retinoic acid. The structural studies provided here were consistent with our prior studies that revealed interactions between the rexinoid and helix 7 residues as a putative "hot-spot" for inducing serum triglyceride synthesis. As proposed in other studies, we believe this occurs by enhancing signaling of RXR:LXR heterodimers in the liver.[9] To lessen toxicity, we also revealed in this study that rexinoid **11** effectively reduced mammary cancers when used at a lower dose and placed in combination with the SERM tamoxifen. The low-dose **11** administration with SERM does not substantially elevate serum triglyceride levels, which is a clinical concern when administering a preventive agent chronically to the high-risk but disease free population.

A surprising find of this study occurred when we changed the isopropyl group at R_1 of the cyclohexenyl ring to a cyclopropyl group. The effectiveness of **10** in cancer prevention was less than **11**, but levels of serum triglycerides were substantially mitigated. While **10** is clearly less potent than **11**, **10** displays similar effectiveness to that of UAB30. On the basis of the results of these studies, UAB30, **10** alone, or **11** in combinations with SERMs appears to offer the most promise for translational development in the prevention of human mammary cancer.

4. EXPERIMENTAL SECTION

^{1}H and ^{13}C NMR spectra were recorded on Bruker ARX 300 or DRX 400 spectrometer. IR spectra were recorded using an ABB Bomem FTIR spectrometer. UV−vis spectra were recorded on a Varian (Carry 100 Conc) spectrophotometer in methanol (Aldrich, spectrograde). Mass spectra were taken on a Hewlett-Packard 1100 LC−MS instrument using electrospray ionization (ESI). Melting points were recorded on an Electrothermal melting point apparatus and are uncorrected. All reactions, unless otherwise mentioned, were monitored by thin layer chromatography (TLC) on 0.25 mm silica gel plates (60F-254, E. Merck or Silicycle). Flash chromatography was performed using Silicycle silica gel (40−63 μm). Reactions and purifications were conducted with nitrogen-saturated solvents and under subdued lighting. Ethyl 4-bromo-3-methylbut-2-enoate (1:1 mixture of isomers) was prepared by the reaction of ethyl 3,3-dimethylacrylate with *N*-bromosuccinimide. Triethyl phosphonosenecioate (1:1 mixture of isomers) was prepared via the Arbusov reaction.[22,23] Triethyl phosphonosenecioate was prepared by using the procedure described in ref 21 except that we used a roughly 1:1 mixture of ethyl 4-bromo-3-methylbut-2-enoate as the starting material. Purity of all the compounds was ≥95%, which was determined by combustion analysis performed by Atlantic Microlabs, Inc. (Norcross, GA).

Reformatsky Reaction for Preparing C15 Acids. By use of this general procedure, all C15 acids were prepared.

(2*Z*)-4-(2′-(3-Methyl)butyl-3′-ethyl-2′-cyclohexen-1′-ylidene)-3-methyl-2-butenoic Acid (17). A suspension of Zn dust (42 g) in 10% HCl (150 mL) was stirred under nitrogen for 10 h in a 1 L, three-neck round bottomed flask. The aqueous layer was decanted, and the zinc was washed successively with distilled water (3 × 150 mL), anhydrous acetone (3 × 150 mL), and anhydrous ether (3 × 150 mL). After removal of the residual ether, the zinc dust was heated strongly with a Bunsen burner flame for about a minute under vacuum. The clumps of zinc were then carefully broken up with a stirring rod. The cooled zinc was suspended in anhydrous dioxane (200 mL), and the stirred suspension was heated to 125 °C in an oil bath. This reaction mixture was then treated dropwise over a period of 1 h with a solution of ketone **13** (47.0 g, 242 mmol) and ethyl 4-bromo-3-methylbut-2-enoate (120 g, 579.43 mmol) in dry dioxane (200 mL). Vigorous bubbling was noticed during the addition process, and the reaction mixture was stirred at reflux for 3 h and then cooled to temperature. Water (100 mL) and 2 N HCl (250 mL) were added. The mixture was diluted with ether (500 mL) and allowed to stir for 15 min. The mixture was filtered, and the acidic layer was separated. The organic layer was washed successively with water (2 × 100 mL), 1 N NaOH (3 × 150 mL). The basic wash was cooled in an ice bath, acidified with HCl (2 N) to pH 1−2, and washed with ether (2 × 200 mL). The combined organic layers were washed with water (2 × 50 mL), brine (50 mL), dried (Na_2SO_4), and evaporated under vacuum to provide a semisolid. This was crystallized from hexanes/ether, filtered, and dried to give 41 g (62%) of pure **17**: mp 71−73 °C; MS *m*/*z* 277 (M + 1); ^{1}H NMR (300 MHz, $CDCl_3$) δ 6.6 (s, 1H), 5.7 (s, 1H), 2.3−2.2 (m, 4H), 2.2−2.1 (m, 4H), 2.1 (s, 3H), 1.7−1.6 (m, 2H), 1.6−1.5 (m, 1H), 1.4−1.3 (m, 2H), 1.0 (t, 3H), 0.9 (d, 6H); ^{13}C NMR ($CDCl_3$) δ 171.1, 157.2, 141.7, 141.2, 132.0, 120.2, 116.9, 38.7, 30.2, 28.8, 28.7, 27.7, 25.9, 25.8, 22.9, 22.5, 12.8.

(2*Z*)-4-(2′-(3-Methyl)butyl-3′-cyclopropyl-2′-cyclohexen-1′-ylidene)-3-methyl-2-butenoic Acid (18). Mp 82−84 °C; MS *m*/*z* 289 (M + 1); ^{1}H NMR (300 MHz, $CDCl_3$) δ 12.0−10.0 (br, 1H), 6.6 (s, 1H), 5.7 (s, 1H), 3.0−2.9 (m, 1H), 2.3−2.2 (m, 4H), 2.1 (s, 3H), 2.1−1.9 (m, 2H), 1.7−1.5 (m, 3H), 1.3−1.2 (m, 2H), 1.0 (d, 6H), 0.9 (d, 6H); ^{13}C NMR ($CDCl_3$) δ 171.9, 157.5, 141.6, 139.4, 134.4, 120.3, 117.3, 38.5, 29.1, 28.9, 26.5, 26.3, 25.9, 23.1, 22.9, 14.7, 5.3.

(2*Z*)-4-(2′-(3-Methyl)butyl-3′-isopropyl-2′-cyclohexen-1′-ylidene)-3-methyl-2-butenoic Acid (19). Mp 100−102 °C; MS *m*/*z* 291 (M + 1); ^{1}H NMR (300 MHz, $CDCl_3$) δ 6.6 (s, 1H), 5.7 (s, 1H), 2.96−2.9 (m, 1H), 2.4−2.2 (m, 4H), 2.1 (s, 3H), 2.1−2.0 (m, 2H) 1.6−1.5 (m, 3H), 1.4−1.3 (m, 2H), 1.0 (d, 6H), 0.9 (d, 6H); ^{13}C NMR ($CDCl_3$) δ 171.8, 157.7, 145.5, 141.8, 131.6, 120.9, 117.4, 39.2, 30.8, 29.3, 29.2, 26.2, 26.0, 24.7, 23.4, 22.9, 21.0.

(2*Z*)-4-(2′-(3-Methyl)butyl-3′-phenyl-2′-cyclohexen-1′-ylidene)-3-methyl-2-butenoic Acid (20). Mp 136−138 °C; MS *m*/*z* 325 (M + 1); ^{1}H NMR (300 MHz, $CDCl_3$) δ 7.4−7.3 (m, 2H), 7.3−7.2 (m, 1H), 7.2−7.1 (m, 2H), 6.7 (s, 1H), 5.7 (s, 1H), 2.44 (t, 2H), 2.37 (t, 2H), 2.2−2.1 (m, 2H), 2.1 (s, 3H), 1.8−1.7 (m, 2H), 1.4−1.2 (m, 3H), 0.7 (d, 6H); ^{13}C NMR ($CDCl_3$) δ 171.9, 157.2, 145.0, 141.1, 140.2, 135.0, 128.5, 128.1, 126.7, 122.7, 117.9, 39.2, 34.2, 28.8, 27.7, 26.9, 26.2, 23.5, 22.7.

General Procedure for the Reduction of C15 Acids. By use of this general procedure, all the alcohols were prepared.

(2*Z*)-4-(2′-(3-Methyl)butyl-3′-ethyl-2′-cyclohexen-1′-ylidene)-3-methyl-2-butenol (21). To a flame-dried three-neck round-bottomed flask fitted with a nitrogen inlet and addition funnel were added acid **17** (40 g, 145 mmol) and anhydrous ether (800 mL). The flask was cooled to 0 °C in an ice bath, and the reaction mixture was treated with 1 M $LiAlH_4$/ether (200 mL, 202 mmol) dropwise. The reaction mixture was stirred for an additional 1 h at 0 °C, cooled to −78 °C in dry ice/acetone bath, and slowly quenched with methanol (100 mL) followed by 10% H_2SO_4 (200 mL). The reaction mixture was allowed to come to room temperature and extracted with ether (3 × 200 mL). The combined ether layers were washed with water (100 mL), brine (2 × 100 mL), dried (Na_2SO_4), and concentrated under vacuum to give the alcohol **21** (38 g,100%) as a colorless oil, which was used in the next reaction without further purification. MS *m*/*z* 263 (M + 1); ^{1}H NMR (300 MHz, $CDCl_3$) δ 5.8 (s, 1H), 5.5−5.4 (m, 1H), 4.0 (d, 2H), 2.3−2.2 (m, 2H), 2.1−2.0 (m, 6H), 1.8 (s, 3H), 1.7−1.5 (m, 3H), 1.3−1.2 (m, 2H), 1.0 (t, 3H), 0.9 (d, 6H); ^{13}C NMR ($CDCl_3$) δ 139.3, 138.1, 137.4, 131.1, 125.3, 119.7, 61.2, 38.9, 30.2, 28.8, 27.9, 27.3, 25.5, 24.2, 23.2, 22.6, 12.9.

(2*Z*)-4-(2′-(3-Methyl)butyl-3′-cyclopropyl-2′-cyclohexen-1′-ylidene)-3-methyl-2-butenol (22). MS *m*/*z* 275 (M + 1); ^{1}H NMR (300 MHz, $CDCl_3$) δ 5.8 (s, 1H), 5.5−5.4 (m, 1H), 4.0 (d, 2H), 2.5−2.4 (m, 2H), 2.1−2.0 (m, 2H), 1.8 (s, 3H), 1.8−1.7 (m, 3H), 1.6−1.5 (m, 3H), 1.4−1.3 (m, 2H), 0.9 (d, 6H), 0.7−0.6 (m, 2H), 0.6−0.5 (m, 2H).

(2*Z*)-4-(2′-(3-Methyl)butyl-3′-isopropyl-2′-cyclohexen-1′-ylidene)-3-methyl-2-butenol (23). MS *m*/*z* 277 (M + 1); ^{1}H NMR (300 MHz, $CDCl_3$) δ 5.8 (s, 1H), 5.5−5.4 (m, 1H), 4.0 (d, 2H), 2.9−2.8

DOI: 10.1021/acs.jmedchem.5b00829
J. Med. Chem. XXXX, XXX, XXX−XXX

(m, 1H), 2.3−2.2 (m, 2H), 2.1−2.0 (m, 4H), 1.8 (s, 3H), 1.6−1.5 (m, 3H), 1.3−1.2 (m, 2H), 1.0 (d, 6H), 0.9 (d, 6H).

(2*Z*)-4-(2′-(3-Methyl)butyl-3′-phenyl-2′-cyclohexen-1′-ylidene)-3-methyl-2-butenol (24). MS *m*/*z* 311 (M + 1); ^{1}H NMR (300 MHz, $CDCl_3$) δ 7.4−7.3 (m, 2H), 7.3−7.2 (m, 1H), 7.2−7.1 (m, 2H), 5.9 (s, 1H), 5.6−5.5 (m, 1H), 4.0 (d, 2H), 2.4−2.3 (m, 2H), 2.3−2.2 (m, 2H), 2.2−2.1 (m, 2H), 1.8 (s, 3H), 1.8−1.7 (m, 3H), 1.3−1.2 (m, 2H), 0.7 (d, 6H).

General Procedure for the Oxidation of Alcohols. By use of this general procedure, all the aldehydes were prepared.

(2*Z*)-4-(2′-(3-Methyl)butyl-3′-ethyl-2′-cyclohexen-1′-ylidene)-3-methyl-2-butenal (25). A three-neck, round-bottomed flask fitted with a reflux condenser was charged with *o*-iodoxybenzoic acid (IBX) (125 g, 446 mmol) and acetone (1000 mL) and warmed to 50−55 °C. A solution of crude alcohol **21** (38 g, 145.0 mmol) in acetone (600 mL) was added all at once to the reaction mixture. The reaction was then allowed to stir at 50−55 °C for 1.5 h under subdued light. The reaction mixture was cooled to 0 °C in an ice bath, diluted with ether (500 mL), and filtered through a sintered glass funnel. The filtrate was washed with ether (2 × 500 mL) and the combined organic layers were concentrated under vacuum (rotary evaporator water bath temperature kept at <35 °C) to give a crude oil. This was purified by flash column chromatography (silica gel, 1:6 ether/hexanes, all column solvents purged with nitrogen) to give pure 9*Z*-aldehyde **25** (27 g (73%) and 0.5 g of all-*E* **25**. MS *m*/*z* 261 (M + 1); ^{1}H NMR (300 MHz, $CDCl_3$) δ 9.5 (d, 1H), 6.0 (s, 1H), 5.95−5.9 (m, 1H), 2.3−2.2 (m, 4H), 2.2−2.1 (m, 4H), 2.0 (s, 3H), 1.7−1.5 (m, 3H), 1.3−1.2 (m, 2H), 1.0 (t, 3H), 0.9 (d, 6H).

(2*Z*)-4-(2′-(3-Methyl)butyl-3′-cyclopropyl-2′-cyclohexen-1′-ylidene)-3-methyl-2-butenal (26). MS *m*/*z* 273 (M + 1); ^{1}H NMR (300 MHz, $CDCl_3$) δ 9.5 (d, 1H), 6.0 (s, 1H), 5.9 (d, 1H), 2.5−2.4 (m, 2H), 2.2−2.1 (m, 2H), 2.0 (s, 3H), 1.8−1.7 (m, 3H), 1.7−1.5 (m, 3H), 1.4−1.3 (m, 2H), 0.9 (d, 6H), 0.8−0.7 (m, 2H), 0.7−0.6 (m, 2H); ^{13}C NMR ($CDCl_3$) δ 193.6, 161.1, 142.5, 140.0, 132.8, 128.5, 117.7, 38.3, 28.7, 28.2, 25.9, 25.7, 25.5, 22.9, 22.6, 14.3, 5.0.

(2*Z*)-4-(2′-(3-Methyl)butyl-3′-isopropyl-2′-cyclohexen-1′-ylidene)-3-methyl-2-butenal (27). MS *m*/*z* 275 (M + 1); ^{1}H NMR (300 MHz, $CDCl_3$) δ 9.5 (d, 1H), 6.0 (s, 1H), 5.9 (d, 1H), 3.0−2.9 (m, 1H), 2.3−2.2 (m, 4H), 2.1 (t, 2H), 2.0 (s, 3H), 1.6−1.5 (m, 3H), 1.3−1.2 (m, 2H), 1.00 (d, 6H), 0.9 (d, 6H); ^{13}C NMR ($CDCl_3$) δ 193.9, 161.5, 146.3, 142.9, 130.4, 128.9, 118.7, 39.4, 30.8, 29.1, 29.0, 25.7, 25.6, 24.8, 23.6, 22.9, 21.1

(2*Z*)-4-(2′-(3-Methyl)butyl-3′-phenyl-2′-cyclohexen-1′-ylidene)-3-methyl-2-butenal (28). MS *m*/*z* 309 (M + 1); ^{1}H NMR (300 MHz, $CDCl_3$) δ 9.6 (d, 1H), 7.4−7.3 (m, 2H), 7.3−7.2 (m, 1H), 7.2−7.1 (m, 2H), 6.1 (s, 1H), 6.0 (d, 1H), 2.4−2.3 (m, 4H), 2.2−2.1 (m, 2H), 2.0 (s, 3H), 1.8−1.7 (m, 2H), 1.4−1.2 (m, 3H), 0.7 (d, 6H); ^{13}C NMR ($CDCl_3$) δ 193.8, 160.9, 144.4, 142.2, 141.9, 133.8, 129.2, 128.6, 127.9, 127.0, 120.6, 39.4, 34.3, 28.8, 28.5, 27.4, 25.7, 23.7, 22.7.

Horner−Emmons Reaction. By use of this general procedure, all the C20 esters were prepared.

(2*E*,4*E*,6*Z*)- and (2*Z*,4*E*,6*Z*)-Ethyl 8-(2′-(3-Methyl)butyl-3′-ethyl-2′-cyclohexen-1′-ylidene)-3,7-dimethyl-2,4,6-octatrienoate (29). To a flame-dried, 2 L, three-neck round-bottomed flask fitted with a nitrogen inlet, addition funnel, and rubber septum was added NaH (60% suspension in mineral oil, 4.96 g, 124.0 mmol). Dry THF (600 mL, distilled over Na/benzophenone) was added to the flask followed by addition of a solution of freshly distilled triethyl phophonosenecioate (33 g, 124.0 mmol). The resulting solution was stirred for 15 min, and then freshly distilled HMPA (87 mL) was added under a nitrogen atmosphere. The flask was covered with aluminum foil and stirred for 15 min. A solution of aldehyde **25** (21.5 g, 82.7 mmol) in dry THF (250 mL) was added dropwise through the addition funnel, and the mixture was then stirred for an additional 1.5 h. The reaction mixture was quenched with water (200 mL) and extracted with ether (3 × 400 mL). The combined ether layers were washed with brine (2 × 250 mL), dried (Na_2SO_4), and concentrated under vacuum to provide the crude product as an oil. The product was purified by chromatography (silica gel; hexanes/ether 8:1) to give 30.0 g of **29** (98%) as an oil (85:15 mixture of (9*Z*):(9*Z*,13*Z*)-**29**). MS *m*/*z* 371 (M + 1); ^{1}H NMR (300 MHz, $CDCl_3$) δ 6.6 (dd, 1H), 6.2 (d, 1H), 6.02 (d, 1H), 5.9 (s, 1H), 5.7 (s, 1H), 4.1 (q, 2H), 2.3−2.2 (m, 2H), 2.2 (s, 3H), 2.2−2.1 (m, 6H), 1.9 (s, 3H), 1.7−1.5 (m, 3H), 1.4−1.3 (m, 2H), 1.3 (t, 3H), 1.0 (t, 3H), 0.9 (d, 6H); ^{13}C NMR ($CDCl_3$) δ 167.3, 153.2, 142.0, 140.0, 138.9, 133.4, 133.1, 131.5, 126.7, 120.1, 118.0, 59.5, 39.0, 30.3, 28.7, 28.4, 27.4, 25.6, 24.8, 23.4, 22.6, 14.4, 13.7, 12.9.

(2*E*,4*E*,6*Z*)- and (2*Z*,4*E*,6*Z*)-Ethyl 8-(2′-(3-Methyl)butyl-3′-cyclopropyl-2′-cyclohexen-1′-ylidene)-3,7-dimethyl-2,4,6-octatrienoate (30). MS *m*/*z* 383 (M + 1); ^{1}H NMR (300 MHz, $CDCl_3$) δ 6.6 (dd, 1H), 6.18 (d, 1H), 6.02 (d, 1H), 5.9 (s, 1H), 5.7 (s, 1H), 4.1 (q, 2H), 2.5−2.4 (m, 2H), 2.2 (s, 3H), 2.1 (t, 2H), 1.9 (s, 3H), 1.8−1.7 (m, 3H), 1.7−1.5 (m, 3H), 1.4−1.3 (m, 2H), 1.3 (t, 3H), 0.9 (d, 6H), 0.7−0.6 (m, 2H), 0.6−0.5 (m, 2H); ^{13}C NMR ($CDCl_3$) δ 167.6, 153.5, 142.4, 139.3, 137.7, 133.8, 133.5, 127.1, 120.0, 118.4, 59.9, 38.9, 29.1, 28.6, 26.3, 26.1, 25.2, 23.4, 23.0, 14.8, 14.6, 14.2, 5.2

(2*E*,4*E*,6*Z*)- and (2*Z*,4*E*,6*Z*)-Ethyl 8-(2′-(3-Methyl)butyl-3′-isopropyl-2′-cyclohexen-1′-ylidene)-3,7-dimethyl-2,4,6-octatrienoate (31). MS *m*/*z* 385 (M + 1); ^{1}H NMR (300 MHz, $CDCl_3$) δ 6.6 (dd, 1H), 6.2 (d, 1H), 6.02 (d, 1H), 5.9 (s, 1H), 5.7 (s, 1H), 4.1 (q, 2H), 3.0−2.9 (m, 1H), 2.3−2.2 (m, 2H), 2.2 (s, 3H), 2.15 (t, 3H), 2.0 (t, 3H), 1.9 (s, 3H), 1.6−1.5 (m, 3H), 1.3−1.2 (m, 5H), 1.0 (d, 6H), 0.9 (d, 6H); ^{13}C NMR ($CDCl_3$) δ 167.6, 153.5, 143.9, 142.4, 139.5, 133.7, 133.5, 130.9, 127.1, 120.6, 118.4, 59.9, 39.6, 30.7, 29.1, 29.0, 25.8, 25.2, 24.8, 23.8, 23.0, 21.2, 14.7, 14.2

(2*E*,4*E*,6*Z*)- and (2*Z*,4*E*,6*Z*)-Ethyl 8-(2′-(3-Methyl)butyl-3′-phenyl-2′-cyclohexen-1′-ylidene)-3,7-dimethyl-2,4,6-octatrienoate (32). MS *m*/*z* 419 (M + 1); ^{1}H NMR (300 MHz, $CDCl_3$) δ 7.4−7.3 (m, 2H), 7.3−7.2 (m, 1H), 7.2−7.1 (m, 2H), 6.7 (dd, 1H), 6.2 (d, 1H), 6.08 (d, 1H), 6.0 (s, 1H), 5.7 (s, 1H), 4.18 (q, 2H), 2.4 (t, 2H), 2.3 (s, 3H), 2.3−2.2 (m, 2H), 2.2−2.1 (m, 2H), 1.95 (s, 3H), 1.8−1.7 (m, 2H), 1.4−1.2 (m, 3H), 1.2 (t, 3H), 0.7 (d, 6H); ^{13}C NMR ($CDCl_3$) δ 167.6, 153.4, 144.9, 141.8, 140.0, 138.5, 134.4, 133.9, 133.5, 128.5, 128.2, 127.5, 126.7, 122.6, 118.6, 60.0, 39.6, 34.3, 28.8, 28.6, 27.5, 25.1, 23.9, 22.8, 14.8, 14.2

General Procedure for Hydrolysis of the Esters. By use of this general procedure, all other C20 acids were prepared.

(2*E*,4*E*,6*Z*)-8-(2′-(3-Methyl)butyl-3′-ethyl-2′-cyclohexen-1′-ylidene)-3,7-dimethyl-2,4,6-octatrienoic Acid (9). The ester **29** (85:15 mixture of (9*Z*):(9*Z*,13*Z*)-**29**) (30.0 g, 81.0 mmol) was suspended in methanol (1300 mL) and warmed to about 70 °C. An aqueous solution of KOH (2.5 N, 325 mL) was added to the above solution and stirred under reflux for 1 h. Then the reaction mixture was cooled in an ice bath, diluted with ice cold water (500 mL), and acidified slowly to pH 2−3 with ice cold 1 N HCl. The resulting yellow precipitate was filtered and washed with ice-cold water. The wet precipitate was dissolved in ether (1000 mL), washed with brine (2 × 200 mL), dried (Na_2SO_4), and concentrated under vacuum to about 100 mL volume. The mixture was diluted with hexanes (200 mL) and cooled in the freezer for 18 h. The resulting yellow crystalline solid was filtered, washed with ice-cold hexanes, and dried to give 16.5 g (59.5%) of pure **9** as single 9*Z* isomer. Mp 119−120 °C; MS *m*/*z* 342 (M + 1); UV λ_{max} 318 nm (ϵ 25 550); ^{1}H NMR (300 MHz, $CDCl_3$) δ 6.6 (dd, 1H), 6.2 (d, 1H), 6.04 (d, 1H), 5.9 (s, 1H), 5.7 (s, 1H), 2.3−2.2 (m, 2H), 2.2 (s, 3H), 2.2−2.1 (m, 6H), 1.9 (s, 3H), 1.6−1.5 (m, 3H), 1.4−1.3 (m, 2H), 1.0 (t, 3H), 0.9 (d, 6H); ^{13}C NMR ($CDCl_3$) δ 172.7, 155.8, 142.9, 140.2, 139.1, 134.4, 132.9, 131.4, 126.7, 120.1, 117.1, 39.0, 30.3, 28.7, 28.4, 27.4, 25.6, 24.9, 23.4, 22.6, 13.9, 12.9.

(2*E*,4*E*,6*Z*)-8-(2′-(3-Methyl)butyl-3′-cyclopropyl-2′-cyclohexen-1′-ylidene)-3,7-dimethyl-2,4,6-octatrienoic Acid (10). Mp 160−162 °C; MS *m*/*z* 355 (M + 1); UV λ_{max} 326 nm (ϵ 22 300); ^{1}H NMR (300 MHz, $CDCl_3$) δ 6.65 (dd, 1H), 6.2 (d, 1H), 6.04 (d, 1H), 5.9 (s, 1H), 5.7 (s, 1H), 2.5−2.4 (m, 2H), 2.2 (s, 3H), 2.15 (t, 2H), 1.9 (s, 3H), 1.8−1.7 (m, 3H), 1.7−1.5 (m, 3H), 1.4−1.3 (m, 2H), 0.9 (d, 6H), 0.7−0.6 (m, 2H), 0.6−0.5 (m2H); ^{13}C NMR ($CDCl_3$) δ 173.2, 156.2, 143.3, 139.5, 137.8, 134.8, 133.8, 133.3, 127.1, 120.0, 117.6, 38.9, 29.1, 28.7, 26.4, 26.1, 25.3, 23.4, 23.1, 14.6, 14.4, 5.2

(2*E*,4*E*,6*Z*)-8-(2′-(3-Methyl)butyl-3′-isopropyl-2′-cyclohexen-1′-ylidene)-3,7-dimethyl-2,4,6-octatrienoic Acid (11). Mp 169−170 °C; MS *m*/*z* 356 (M + 1); UV λ_{max} 328 nm (ϵ 25 900); ^{1}H NMR (300 MHz, $CDCl_3$) δ 6.6 (dd, 1H), 6.2 (d, 1H), 6.04 (d, 1H), 5.9 (s, 1H), 5.7 (s, 1H), 3.0−2.9 (m, 1H), 2.3−2.2 (m, 2H), 2.2 (s, 3H), 2.1 (t,

DOI: 10.1021/acs.jmedchem.5b00829
J. Med. Chem. XXXX, XXX, XXX−XXX

2H), 2.0 (t, 2H), 1.9 (s, 3H), 1.6−1.5 (m, 3H), 1.3−1.2 (m, 2H), 1.0 (d, 6H), 0.9 (d, 6H); ^{13}C NMR ($CDCl_3$) δ 173.2, 156.2, 144.1, 143.4, 139.8, 134.7, 133.3, 130.9, 127.1, 120.6, 117.6, 39.6, 30.7, 29.1, 29.0, 25.8, 25.3, 24.8, 23.8, 23.0, 21.2, 14.4

(2*E*,4*E*,6*Z*)-8-(2′-(3-Methyl)butyl-3′-phenyl-2′-cyclohexen-1′-ylidene)-3,7-dimethyl-2,4,6-octatrienoic Acid (12). Mp 168−169 °C; MS m/z 391 (M + 1); UV λ_{max} 328 nm (ϵ 26 300); ^{1}H NMR (300 MHz, $CDCl_3$) δ 7.4−7.3 (m, 2H), 7.3−7.2 (m, 1H), 7.2−7.1 (m, 2H), 6.7 (dd, 1H), 6.24 (d, 1H), 6.1 (d, 1H), 6.0 (s, 1H), 5.8 (s, 1H), 2.4 (t, 2H), 2.3 (s, 3H), 2.3−2.2 (m, 2H), 2.2−2.1 (m, 2H), 1.97 (s, 3H), 1.8−1.7 (m, 2H), 1.4−1.3 (m, 3H), 0.7 (d, 6H); ^{13}C NMR ($CDCl_3$) δ 173.1, 156.1, 144.9, 142.7, 140.1, 138.7, 134.5, 134.4, 133.7, 128.5, 128.2, 127.5, 126.8, 122.5, 117.8, 39.6, 34.3, 28.8, 28.6, 27.6, 25.2, 23.9, 22.8, 14.5.

Binding Affinity, Transient Transfection, and Luciferase Reporter Assays. The binding affinity of **1**−**12** to hRXRα-LBD homodimer was measured using a fluorescence quenching method.[24] hRXRα-LBD homodimers (0.5 μM) were excited at 280 nm, and the protein fluorescence was measured at 337 nm with a Cary Eclipse fluorescence spectrophotometer (Varian, Palo Alto, CA). The binding association constant K_a was calculated by using a nonlinear least-squares regression to fit the raw data.[24]

Transient transfection and luciferase reporter assays were performed using a previously reported protocol.[25] At 24 h prior to transfection, human embryonic kidney (HEK) 293 cells were plated at 2×10^5 cells per well in six-well plates. Transfection mixtures included 0.2 μg of the Gal4 reporter plasmid pGL4.31[luc2P/Gal4UAS/Hygro] (Promega), 0.5 μg of pCMXGal4-hRARα or pCMX-Gal4-hRXRα expression vector, and 0.01 μg of Renilla luciferase reporter plasmid, pRL-TK. TransIT-LT1 transfection reagent (Mirus) was used. At 24 h post-transfection, rexinoid was added to the culture medium. At 48 h post-transfection, reporter activity was determined using the dual luciferase reporter assay (Promega). The EC_{50} of the hRXRα luciferase assay was determined using a dose response model with triplicates at four different concentrations (1, 10, 100, 1000 nM). A single 1000 nM dose of rexinoid was used to evaluate the percentage of hRARα activation using the same concentration of 9-*cis*-retinoic acid as the positive 100% control.

Isothermal Titration Calorimetry of GRIP-1 Binding to holo-hRXRα-LBD. A Microcal VP-Isothermal titration calorimeter (Microcal, Piscataway, NJ) was used to measure binding of the GRIP-1 coactivator peptide to holo-hRXRα-LBD homodimers as described previously.[1] Each titration experiment consisted of 30 injections of 8 μL of GRIP-1 peptide (0.04−0.12 mM) into the sample cell containing 1.34 mL of hRXRα-LBD homodimers (0.05 mM) in 10 mM Tris buffer (pH 8.0) containing 50 mM NaCl, 0.5 mM EDTA, and 2 mM DTT. Rexinoids **11** or **12** were dissolved in DMSO and added at a ratio of 2:1 (retinoid:protein). Both retinoid solution and hRXRα-LBD solution were degassed at least 15 min before the rexinoids were added to the protein solution. The ITC data were processed using the ORIGIN 7 software. The titration curves were fit to a single site binding model by a nonlinear least-squares method. The ITC experiments were performed at 37 °C.

In Vivo Triglyceride Levels Assay. All animal studies were performed in accordance with the University of Alabama at Birmingham guidelines as defined by the Institutional Animal Care and Use Committee (IACUC-121008309). The triglyceride assays were conducted on female Sprague-Dawley rats bearing small mammary cancers. Mammary cancers were induced in 50-day-old female Sprague-Dawley rats by iv injection of the chemical carcinogen methylnitrosourea (75 mg/kg BW). The animals were fed a Teklad diet according to previous reports.[3] The retinoids tested were mixed into the diet according to the protocols reported previously and fed for 7 days.[3] For the evaluation of the compounds on serum triglycerides, blood was collected from the inferior vena cava at the time of sacrifice of the animals. The blood was kept at 5 °C during centrifugation (3800 rpm for 15 min). Serum was immediately collected and frozen at −85 °C until analyzed for triglycerides.[26] The infinity triglycerides assay kit was purchased from Thermo DMA.

Protein Purification, Crystallization, and X-ray Crystallography. The hRXRα-LBD (T_{223}−T_{462}) was overexpressed in *Escherichia coli* and purified using AKTA purifier system.[1] The hRXRα-LBD homodimers were isolated from a gel filtration chromatography. The protein was mixed with a 4-fold excess of UAB rexinoids and then 5-fold excess of GRIP-1 coactivator peptide. The ternary complexes were crystallized using vapor diffusion technique in hanging drops.[1] Diffraction data of crystals were collected at synchrotron source of Advanced Proton Source (APS) at Argonne National Laboratory. The collected diffraction data were processed using the program HKL2000. The structures were solved using the molecular replacement method with a high-resolution hRXRα-LBD structure with its ligand deleted as a search model (PDB code 3OAP). The structures were refined using CNS software.[27] A complete summary of data for these structures is given in a Supporting Information table. Interactions between ligand/peptide and hRXRα-LBD were analyzed using a program Ligand-Protein Contacts (LPC)/Contacts of Structural Units (CSU).[28] All structures were prepared using PyMol (*The PyMOL Molecular Graphics System*, version 0.99; Schrödinger, LLC: New York.).

■ ASSOCIATED CONTENT

Supporting Information

The Supporting Information is available free of charge on the ACS Publications website at DOI: 10.1021/acs.jmedchem.5b00829.

Synthesis of compounds **6**−**8** and intermediates **13**−**16**, tables containing the crystallographic data, refinement statistics, and elemental analysis data (PDF)

Molecular formula strings (XLSX)

Accession Codes

PDB codes: compound **6**, 4RFW; compound **9**, 4RMC; compound **10**, 4RMD; compound **11**, 4RME.

■ AUTHOR INFORMATION

Corresponding Authors

*W.J.B.: phone, 1-205-934-8288; fax, 1-205-934-2543; e-mail, wbrou@uab.edu.

*D.D.M.: phone, 1-205-934-8285; fax, 1-205-934-2543; e-mail, muccio@uab.edu.

Notes

The authors declare no competing financial interest.

■ ACKNOWLEDGMENTS

We thank Dr. Ellen Li (Washington University in St. Louis, MO) for providing the protein expression vector. We appreciate critical reading and helpful comments provided by Dr. Debasish Chattopadhyay. This work was supported by the National Institutes of Health (NIH) Grant 2 P50 CA089019, the Komen Foundation (Grant BCTR 20000690), and Grant RO1AA12153.

■ ABBREVIATIONS USED

RXR, retinoid X receptor; RAR, retinoic acid receptor; RA, retinoic acid; LBD, ligand binding domain; IBX, *o*-iodoxybenzoic acid; HEK293, human embryonic kidney cell; TG, triglycerides; GRIP-1, glucocorticoid receptor interacting peptide 1; LBP, ligand binding pocket; MNU-1, methyl-1-nitrosourea; ER, estrogen receptor; SERM, selective estrogen receptor modulator; THF, tetrahydrofuran; HMPA, hexamethylphosphoramidate; TLC, thin layer chromatography

■ REFERENCES

(1) Xia, G.; Boerma, L. J.; Cox, B. D.; Qiu, C.; Kang, S.; Smith, C. D.; Renfrow, M. B.; Muccio, D. D. Structure, energetics, and dynamics of binding coactivator peptide to the human retinoid X receptor alpha

DOI: 10.1021/acs.jmedchem.5b00829
J. Med. Chem. XXXX, XXX, XXX−XXX

ligand binding domain complex with 9-cis-retinoic acid. *Biochemistry* **2011**, *50*, 93−105.
(2) Boerma, L. J.; Xia, G.; Qui, C.; Cox, B. D.; Chalmers, M. J.; Smith, C. D.; Lobo-Ruppert, S.; Griffin, P. R.; Muccio, D. D.; Renfrow, M. B. Defining the Communication between Agonist and Coactivator Binding in the Retinoid X Receptor alpha Ligand Binding Domain. *J. Biol. Chem.* **2014**, *289*, 814−26.
(3) Grubbs, C. J.; Lubet, R. A.; Atigadda, V. R.; Christov, K.; Deshpande, A. M.; Tirmal, V.; Xia, G.; Bland, K. I.; Eto, I.; Brouillette, W. J.; Muccio, D. D. Efficacy of new retinoids in the prevention of mammary cancers and correlations with short-term biomarkers. *Carcinogenesis* **2006**, *27*, 1232−1239.
(4) Muccio, D. D.; Brouillette, W. J.; Breitman, T. R.; Taimi, M.; Emanuel, P. D.; Zhang, X.; Chen, G.; Sani, B. P.; Venepally, P.; Reddy, L.; Alam, M.; Simpson-Herren, L.; Hill, D. L. Conformationally defined retinoic acid analogues. 4. Potential new agents for acute promyelocytic and juvenile myelomonocytic leukemias. *J. Med. Chem.* **1998**, *41*, 1679−87.
(5) Atigadda, V. R.; Vines, K. K.; Grubbs, C. J.; Hill, D. L.; Beenken, S. L.; Bland, K. I.; Brouillette, W. J.; Muccio, D. D. Conformationally defined retinoic acid analogues. 5. Large-scale synthesis and mammary cancer chemopreventive activity for (2E,4E,6Z,8E)-8(3′,4′-dihydro-1′(2′H)-naphthalen-1′-ylidene)-3,7-dimethyl-2,4,6-octatrienoic acid (9cUAB30). *J. Med. Chem.* **2003**, *46*, 3766−3769.
(6) Duvic, M.; Martin, A. G.; Kim, Y.; Olsen, E.; Wood, G. S.; Crowley, C. A.; Yocum, R. C.; Worldwide Bexarotene Study Group.. Phase 2 and 3 clinical trial of oral bexarotene (Targretin capsules) for the treatment of refractory or persistent early-stage cutaneous T-cell lymphoma. *Arch. Dermatol.* **2001**, *137*, 581−93.
(7) Miller, V. A.; Benedetti, F. M.; Rigas, J. R.; Verret, A. L.; Pfister, D. G.; Straus, D.; Kris, M. G.; Crisp, M.; Heyman, R.; Loewen, G. R.; Truglia, J. A.; Warrell, R. P., Jr. Initial clinical trial of a selective retinoid X receptor ligand, LGD1069. *J. Clin Oncol* **1997**, *15*, 790−5.
(8) Grubbs, C. J.; Hill, D. L.; Bland, K. I.; Beenken, S. W.; Lin, T. H.; Eto, I.; Atigadda, V. R.; Vines, K. K.; Brouillette, W. J.; Muccio, D. D. 9cUAB30, an RXR specific retinoid, and/or tamoxifen in the prevention of methylnitrosourea-induced mammary cancers. *Cancer Lett.* **2003**, *201*, 17−24.
(9) Vedell, P. T.; Lu, Y.; Grubbs, C. J.; Yin, Y.; Jiang, H.; Bland, K. I.; Muccio, D. D.; Cvetkovic, D.; You, M.; Lubet, R. Effects on gene expression in rat liver after administration of RXR agonists: UAB30, 4-methyl-UAB30, and Targretin (Bexarotene). *Mol. Pharmacol.* **2013**, *83*, 698−708.
(10) Desphande, A.; Xia, G.; Boerma, L. J.; Vines, K. K.; Atigadda, V. R.; Lobo-Ruppert, S.; Grubbs, C. J.; Moeinpour, F. L.; Smith, C. D.; Christov, K.; Brouillette, W. J.; Muccio, D. D. Methyl-substituted conformationally constrained rexinoid agonists for the retinoid X receptors demonstrate improved efficacy for cancer therapy and prevention. *Bioorg. Med. Chem.* **2014**, *22*, 178−85.
(11) Atigadda, V. R.; Xia, G.; Desphande, A.; Boerma, L. J.; Lobo-Ruppert, S.; Grubbs, C. J.; Smith, C. D.; Brouillette, W. J.; Muccio, D. D. Methyl substitution of a rexinoid agonist improves potency and reveals site of lipid toxicity. *J. Med. Chem.* **2014**, *57*, 5370−80.
(12) Muccio, D. D.; Brouillette, W. J.; Alam, M.; Vaezi, M. F.; Sani, B. P.; Venepally, P.; Reddy, L.; Li, E.; Norris, A. W.; Simpson-Herren, L.; Hill, D. L. Conformationally defined 6-s-trans-retinoic acid analogs. 3. Structure-activity relationships for nuclear receptor binding, transcriptional activity, and cancer chemopreventive activity. *J. Med. Chem.* **1996**, *39*, 3625−35.
(13) Alam, M.; Zhestkov, V.; Sani, B. P.; Venepally, P.; Levin, A. A.; Kazmer, S.; Li, E.; Norris, A. W.; Zhang, X. K.; Lee, M. O.; Hill, D. L.; Lin, T. H.; Brouillette, W. J.; Muccio, D. D. Conformationally Defined 6-S-Trans-Retinoic Acid Analogs. 2. Selective Agonists for Nuclear Receptor-Binding and Transcriptional Activity. *J. Med. Chem.* **1995**, *38*, 2302−2310.
(14) Frigerio, M.; Santagostino, M.; Sputore, S. A user-friendly entry to 2-iodoxybenzoic acid (IBX). *J. Org. Chem.* **1999**, *64*, 4537−4538.
(15) Lu, Y.; You, M.; Ghazoui, Z.; Liu, P.; Vedell, P. T.; Wen, W.; Bode, A. M.; Grubbs, C. J.; Lubet, R. A. Concordant effects of aromatase inhibitors on gene expression in ER+ Rat and human mammary cancers and modulation of the proteins coded by these genes. *Cancer Prev. Res.* **2013**, *6*, 1151−61.
(16) den Hollander, P.; Savage, M. I.; Brown, P. H. Targeted therapy for breast cancer prevention. *Front. Oncol.* **2013**, *3*, 250.
(17) Kedishvili, N. Y. Enzymology of retinoic acid biosynthesis and degradation. *J. Lipid Res.* **2013**, *54*, 1744−60.
(18) Uray, I. P.; Shen, Q.; Seo, H. S.; Kim, H.; Lamph, W. W.; Bissonnette, R. P.; Brown, P. H. Rexinoid-induced expression of IGFBP-6 requires RARbeta-dependent permissive cooperation of retinoid receptors and AP-1. *J. Biol. Chem.* **2009**, *284*, 345−53.
(19) Bonofiglio, D.; Cione, E.; Qi, H.; Pingitore, A.; Perri, M.; Catalano, S.; Vizza, D.; Panno, M. L.; Genchi, G.; Fuqua, S. A.; Ando, S. Combined low doses of PPARgamma and RXR ligands trigger an intrinsic apoptotic pathway in human breast cancer cells. *Am. J. Pathol.* **2009**, *175*, 1270−80.
(20) Papi, A.; De Carolis, S.; Bertoni, S.; Storci, G.; Sceberras, V.; Santini, D.; Ceccarelli, C.; Taffurelli, M.; Orlandi, M.; Bonafe, M. PPARgamma and RXR ligands disrupt the inflammatory cross-talk in the hypoxic breast cancer stem cells niche. *J. Cell. Physiol.* **2014**, *229*, 1595−606.
(21) Kong, G.; Kim, H. T.; Wu, K.; DeNardo, D.; Hilsenbeck, S. G.; Xu, X. C.; Lamph, W. W.; Bissonnette, R.; Dannenberg, A. J.; Brown, P. H. The retinoid X receptor-selective retinoid, LGD1069, down-regulates cyclooxygenase-2 expression in human breast cells through transcription factor crosstalk: implications for molecular-based chemoprevention. *Cancer Res.* **2005**, *65*, 3462−9.
(22) Herz, W. Azulenes. VII. Novel Rearrangement in the Synthesis of Azulenes. *J. Am. Chem. Soc.* **1956**, *78*, 1485−1494.
(23) Gedye, R. N.; Westaway, K. C.; Arora, P.; Bisson, R.; Khalil, A. The stereochemistry of the Wittig reactions of alllylic phosphoranes and phosphonate esters with aldehydes. *Can. J. Chem.* **1977**, *55*, 1218−1228.
(24) Cheng, L.; Norris, A. W.; Tate, B. F.; Rosenberger, M.; Grippo, J. F.; Li, E. Characterization of the Ligand-Binding Domain of Human Retinoid-X Receptor-Alpha Expressed in Escherichia coli. *J. Biol. Chem.* **1994**, *269*, 18662−18667.
(25) Jiang, W.; Deng, W.; Bailey, S. K.; Nail, C. D.; Frost, A. R.; Brouillette, W. J.; Muccio, D. D.; Grubbs, C. J.; Ruppert, J. M.; Lobo-Ruppert, S. M. Prevention of KLF4-mediated tumor initiation and malignant transformation by UAB30 rexinoid. *Cancer Biol. Ther.* **2009**, *8*, 289−98.
(26) McGowan, M. W.; Artiss, J. D.; Strandbergh, D. R.; Zak, B. A peroxidase-coupled method for the colorimetric determination of serum triglycerides. *Clin. Chem.* **1983**, *29*, 538−42.
(27) Brunger, A. T.; Adams, P. D.; Clore, G. M.; DeLano, W. L.; Gros, P.; Grosse-Kunstleve, R. W.; Jiang, J. S.; Kuszewski, J.; Nilges, M.; Pannu, N. S.; Read, R. J.; Rice, L. M.; Simonson, T.; Warren, G. L. Crystallography & NMR system: A new software suite for macromolecular structure determination. *Acta Crystallogr., Sect. D: Biol. Crystallogr.* **1998**, *54*, 905−921.
(28) Sobolev, V.; Sorokine, A.; Prilusky, J.; Abola, E. E.; Edelman, M. Automated analysis of interatomic contacts in proteins. *Bioinformatics* **1999**, *15*, 327−32.

DOI: 10.1021/acs.jmedchem.5b00829
J. Med. Chem. XXXX, XXX, XXX−XXX